Bull. Mater. Sci., Vol. 32, No. 1, February 2009, pp. 65–76. © Indian Academy of Sciences.

Influence of fibre-surface treatment on structural, thermal and mechanical properties of jute fibre and its composite

E SINHA* and S K ROUT†

Department of Physics, National Institute of Technology, Rourkela 769 008, India
†Department of Applied Physics, Birla Institute of Technology, Ranchi 835 215, India

MS received 20 November 2007

Abstract. **Jute fibres (*Corchorus olitorious*), an environmentally and ecologically friendly product, were chemically modified and treated with 5% NaOH solution at room temperature for 2 h, 4 h and 8 h. The above samples were characterized and morphologically analysed by X-ray diffraction (XRD), Fourier transform infrared spectroscopy (FT–IR), differential scanning calorimetry (DSC), scanning electron microscopy (SEM) and Instron 1185. Alkali treatment affects the supramolecular structure of the fibre as shown by XRD by improving the degree of crystallinity of the fibre. Surface chemistry of the fibre also altered as depicted by FT–IR studies. This chemical treatment was also found to alter the characteristic of the fibre surface topography as seen by the SEM. From the mechanical single fibre test it was found that the tenacity and modulus of the fibre improved after alkali treatment. This might be due to the improvement in the crystallinity. DSC data demonstrated that the thermal degradation temperature for the cellulose get lowered from 365·26°C to 360·62°C after alkali treatment led to the reduction in fibre thermal stability. Jute fibre reinforced composite were prepared with treated and untreated jute fibre (15 wt%) reinforced unsaturated polyester (UPE). Effectiveness of these composites was experimentally investigated through the study of the composites by DSC, Instron 1195 for mechanical property of composites, volume fraction of the porosity and hydrophobic finishing of the composite. From the DSC analysis it was found that thermal stability enhanced for treated fibre reinforced composite. This could be due to the resistance offered by the closely packed cellulose chain in combination with the resin. Flexural strength of the composite prepared with 2 h and 4 h alkali treated fibre were found to increase by 3·16% and 9·5%, respectively. Although 8 h treated fibre exhibited maximum strength properties, but the composite prepared with them showed lower strength value. Alkali treatment helped in the development of hydrophobicity and reduction in volume fraction of the porosity. This may be due to the better fibre matrix interface adhesion caused due to the fibre surface treatment by alkali.**

Keywords. **Jute fibre; composites; mechanical properties; thermal properties.**

1. Introduction

During the past decade, increasing environmental awareness, new global agreements and international governmental policies and regulations have been the driving force behind the renewed interest in the natural fibres. The attractiveness of a plant-based fibre comes from its high specific strength and stiffness, natural availability and environmental 'friendliness'. Natural cellulose-based fibres are gaining increasing attention for their diversified applications in engineering and their uses, such as building materials and structural parts for the automotive application, where light weight is required. Low cost and less tool wear during processing are among the known advantages of the plant-fibres. The approximate chemical composition of the jute fibre (Khan and Ahmed 1996) in weight % is: cellulose (58–63), hemicelluloses (20–22), lignin (12–15), small amounts of protein (2%), mineral matter (1%) and trace quantities of organic and inorganic pigments. The elementary units of cellulose macromolecules are anhydro-*d*-glucose which contains three hydroxyls (–OH) (Khan and Ahmed 1996). These hydroxyls form the hydrogen bonds inside the macromolecule itself (intramolecular) and between the other cellulose macromolecules (intermolecular) as well. Therefore, all vegetable fibres are hydrophilic in nature, and their moisture contents can reach up to 3–13% (Bledzki *et al* 1996), which is one of the reasons for the degradation of the fibres. Although, as with most of the other plant-based natural fibres, cellulose forms the main structural components, lignin and hemicelluloses also play an important part in determining the characteristic properties of the fibres. Jute hemicelluloses, which are thought to consist principally of xylan, polyuronide and hexosan have been shown to be very sensitive to the action of caustic soda,

*Author for correspondence (elasinha@gmail.com)

which also exerts some effects on lignin or α-cellulose (McMillan *et al* 1954). Several authors have employed the technique of mercerization for jute and the changes occurring in the fibre properties have been investigated. Sarkar (1935) treated jute fibres with NaOH solution of concentration 1 and 8% for 48 h and observed 130% improvement in the tensile strength of the fibres in both the cases. Similarly, jute fibres were treated with 2% NaOH solution for 1 h by Samal *et al* (1995) and 13% improvement in the tenacity of the fibres was reported. It is observed that coir fibre when alkali treated at 5% NaOH for 72–96 h showed improvement in tensile strength by 10–15% and modulus by 40% (Prasad *et al* 1983). Rout (1999) reported improvement of 35% in tensile strength, 60% in flexural strength and 69% in impact strength of the composites containing 5% alkali treated reinforced natural fibres.

In the present investigation, an effort was made to study the supramolecular structure, morphological and surface chemistry of the fibre by XRD, SEM and FT–IR of untreated and 5% alkali-treated jute fibres for 2, 4 and 8 h and correlate these studies to its thermal and some mechanical properties. Fibres after being analysed by above mentioned studies is compared with some properties of its composite prepared by 15 weight % of fibre reinforced unsaturated polyester (UPE) resin. Thermal analysis by DSC, flexural mechanical property analysis by Instron 1195, volume fraction of porosity and water uptake capacity were analysed to characterize these composites.

2. Experimental

2.1 *Materials*

Jute fibres (*Corchorus olitorius*) were collected from the Central Research Institute of Jute and Allied Fibre (CRIJAF), Kolkata. Collected fibres were dewaxed in a mixture of alcohol and benzene (1 : 2) as done by Roy (1960). As a result of this treatment, the specimen attains a 'hohlraum' character (according to Porod (1953) and Ratho *et al* (1970)), i.e. the substance occurs in layers like the pages of a book with free space in between. This is treated as a raw sample in this study. Unsaturated polyester resin was used as matrix and its curing characteristics were enhanced by the use of 1·5% hardener and 2% accelerator.

2.2 *Alkali treatment*

The jute fibres were cut to 50 cm of length and were soaked in a 5% NaOH solution at 30°C for 2, 4 and 8 h. The fibres were then washed several times with distilled water to remove any NaOH sticking to the fibre surface, neutralized with dilute acetic acid and washed again with distilled water. Final pH maintained was 7·0. The fibres were then dried at room temperature for 48 h, followed by oven drying at 100°C for 6 h for the removal of moisture content. The 5% alkali-treated fibres for 2 h, 4 h and 8 h are regarded as M jute 2 h, M jute 4 h and M jute 8 h, respectively, hereafter.

2.3 *Fibre fineness determination*

The weight changes of the fibres after different treatments were determined by % weight loss calculated as

$$\%\text{Weight loss} = \frac{(W_1 - W_2)}{W_1} \times 100, \quad (1)$$

where W_1 was the weight of fixed amount of dry raw jute fibres whereas W_2 was the weight of dry fibres after being treated. Fibre fineness was determined in terms of linear density in accordance with ASTM D1577-92. The linear density was calculated on the basis of the weight of 100 single fibres of 60 mm length each and converted into tex.

2.4 *Composite fabrication methods*

The matrix materials were prepared from commercially available general purpose unsaturated-polyester resin, accelerator and hardener in a weight ratio of 1 : 0·02 : 0·015, respectively. A simple hand lay-up technique had been used for the preparation of the specimens. Each layer of the fibre were pre-impregnated with matrix materials and placed one over the other in the mould, taken care to maintain practically achievable tolerances on fibre alignment. Arrangements were made to avoid the leakage of matrix material by keeping the two opposite ends open to allow hot air to escape during curing at room temperature and post curing by oven heating at 60°C for 8 h. The composite was prepared with 15 weight % of fibre and was constant for all the specimens.

2.4a *Flexural 3-point bend test specimen*: Unidirectional oriented raw jute fibre and alkali-treated jute fibre reinforced polyester composites were prepared in accordance with ASTMD790 for this test.

2.4b *Hydrophobicity test specimen*: Unidirectional oriented raw jute fibre and alkali-treated jute fibre reinforced polyester composites of dimension 13·7 × 2·3 × 0·48 cm were prepared. Hydrophobicity test samples were cut by hack saw to length 3 cm and width 2 cm. The thickness was controlled by keeping the weight % of the fibre and matrix constant for all the samples.

2.4c *Porosity determination specimen*: Unidirectional oriented raw jute fibre and alkali-treated jute fibre reinforced polyester composites of dimension 13·7 ×

2·3 × 0·48 cm were prepared. Test samples were cut by hack saw of length 42 mm, width 6·5 mm and thickness 4·8 mm.

2.5 *Characterization of fibres*

2.5a *Scanning electron microscope (SEM)*: The scanning electron micrographs of fibre samples were taken in Hitachi (S-3400N) SEM. The samples were coated with a 20 nm thick gold layer.

2.5b *Fourier transform infrared (FTIR)*: The raw and alkali treated jute fibres were analysed by FT–IR spectroscopy. Room-temperature FT–IR spectra were recorded on solid samples in KBr pellets by means of a Shimadzu FT–IR spectrometer (IR Prestige-21) with a resolution of 4 cm^{-1}. The spectra were smoothened with a constant smooth factor for comparison.

2.5c *X-ray diffraction*: 2.5c(i) *Principle*: The strains developed in the crystallites due to treatment manifest as change in lattice planes, causing line shifting. These changes in the lattice planes are measured by X-ray diffraction method. Microstress causes diffraction line broadening, while macrostress causes line shifting. The relation between the broadening produced and the non-uniformity of the strain can be verified by differentiating the Bragg law. The spacing, d, of a set of planes in a crystal is related to the Bragg angle, θ, and the wavelength, λ, by the equation

$$d = \frac{\lambda}{2\sin\theta}. \tag{2}$$

The expression for change in d due to irradiation can be measured by noting the change in θ. Differentiating d with respect to θ, we have

$$\frac{\Delta d}{\Delta\theta} = \frac{1}{2}\lambda \operatorname{cosec}\theta.\cot\theta \tag{3}$$

$$= -d\cot\theta$$

$$\text{or} \quad \frac{\Delta d}{d} = -\cot\theta.\Delta\theta\,. \tag{4}$$

Since diffraction angle is measured in terms of 2θ, then

$$\frac{\Delta d}{d} = -\cot\theta.\Delta 2\theta/2$$

$$\Rightarrow \Delta 2\theta = -2\frac{\Delta d}{d}\tan\theta. \tag{5}$$

Hence,

$$b = \Delta 2\theta = -2\frac{\Delta d}{d}\tan\theta, \tag{6}$$

where b is the extra broadening, over and above the instrumental breadth of the line due to a fractional variation in plane spacing $\Delta d/d$ to be calculated from the observed broadening.

If d_i indicates the non-treated (unstressed) spacing and d_s the spacing in the treated (strained) fibre, the microstrain in the particles in the direction normal to the diffracting plane is

$$\varepsilon = \frac{\Delta d}{d} = \left(\frac{d_s - d_u}{d_u}\right). \tag{7}$$

If $d_s > d_u$, then $\Delta d/d$ is positive which indicates that the residual stress is tensile and if $d_s < d_u$, then $\Delta d/d$ is negative indicating generation of residual compressive stress in the surface. This value of $\Delta d/d$, however, includes both tensile and compressive strains. Assuming both are equal for micro-crystallites, the value of $\Delta d/d$ must be divided by two to obtain the maximum tensile strain alone, or maximum compressive strain alone (Cullity 1978). Again, maximum microstress present in the sample can be defined as

$$\sigma_{\text{stress}} = \frac{\varepsilon}{2}E. \tag{8}$$

Putting the value of ε, we obtain

$$\sigma_{\text{stress}} = \frac{1}{2}\frac{\Delta d}{d}E, \tag{9}$$

where E is the elastic constant or generally known as Young's modulus of the material.

The crystallite size of the samples were calculated using well known Scherrer formula (Cullity 1978)

$$t = \frac{k\lambda}{\beta\cos\theta}, \tag{10}$$

where $\beta(= B - b)$ is the FWHM; B the line width; b the instrumental broadening; K the shape factor (= 0·89); θ the Bragg angle and λ the wavelength of $CuK_{\alpha 1}$ (1·54056). The factor, 57·3, is used to convert the value of β from degree to radians to obtain the particle size in nm or angstrom unit. The crystallinity index (CrI) of the fibres was calculated according to the Segal empirical method as follows (Segal *et al* 1959)

$$\text{CrI}(\%) = \left(\frac{I_{002} - I_{\text{am}}}{I_{002}}\right) \times 100, \tag{11}$$

where I_{002} is the maximum intensity of the 002 lattice reflection of the cellulose crystallographic form (I) at $2\theta \sim 22{\cdot}5°$ and I_{am} the intensity of diffraction of the amorphous material at $2\theta \sim 16{\cdot}2°$.

2.5c(ii) *Experimental techniques*: For X-ray diffraction, appropriate amounts of jute fibre were taken, cut

into small pieces and grinded in an agate motor. The jute powders were compressed to form a pellet of diameter 15mm. The X-ray diffraction data were collected using a Philips Analytical X-ray Instrument, X'Pert-MPD (PW 3020 vertical goniometer and 3710 MPD control unit) employing Bragg–Brentano parafocusing optics. The XRD patterns were recorded with a step size of 0·01° on a 5–50° range with a scanning rate of 2° per min. Line focus Ni-filtered CuK$_\alpha$ radiation from an X-ray tube (operated at 40 kV and 30 mA) was collimated through soller slit (SS) of 0·04 rad., fixed divergence slit of 1° and mask (5 mm) before getting it diffracted from the sample. Then the diffracted beam from the sample was well collimated by passing it through a programmable anti-scattering slit off 1° to reduce air scattering, programmable receiving slit of 0·3 mm and soller slit of 0·04 rad. before getting it reflected by the curved graphite crystal (002) monochromater of radius 225 mm for high resolution diffraction study. A Xe-gas filled proportional counter (PW1711/90) with electronic pulse height discrimination was mounted on the arm of the goniometer circle of radius 200 mm to receive diffracted X-ray signal. Experimental control and data acquisition were fully automated through computer.

2.5d *Mechanical properties analysis of fibre*: Single fibre tensile tests were carried out using an Instron 1185 at the National Institute of Research on Jute and Allied Fibre Technology (NIRJAFT), Kolkata. A gauge length of 10 mm was employed with a cross-head speed of 5 mm/min. Fifty single fibres each of length 50 mm of raw and treated fibre were tested.

2.5e *Thermal analysis of fibre*: DSC measurements were performed using a (TA Instrument, USA, Model No. Q10) thermal analyser. A heating rate of 10°C/min and a sample weight of 3–4 mg in an aluminium crucible with a pin hole were used in a nitrogen atmosphere (50 ml/min).

2.6 *Composite characterization*

2.6a *Test for hydrophobicity*: The composite was prepared at room temperature and finally conditioned at 50°C for 12 h for the determination of final conditioned weight (W_1). Subsequently, the conditioned samples were immersed in distilled water for 24 h, dried and finally the immersed weight (W_2) was determined since there were no soluble components in the sample. Percentage of water absorbed was calculated as follows (Mohanty *et al* 2004). Three test specimens were studied for each set and were averaged.

$$\text{Water uptake} = \frac{(W_2 - W_1)}{W_1} \times 100. \tag{12}$$

2.6b *Determination of volume fraction of porosity, V_p in composites*: The laminate volume, V_c, of the specimens were calculated based on the average values of the thickness, t_c, the length, l_c and the width, b_c, where the subscript c denotes composite.

$$V_c = t_c \times b_c \times l_c. \tag{13}$$

The fibre weights in the laminates, W_f, were calculated from the weight of the fibre, $W_{f,start}$, in the prepared laminate with fibre length, $l_{f,start}$. The fibre length was reduced from $l_{f,start}$ to l_c, when the laminates were cut into specimen length where the subscript, f, denotes fibre. In our case, the dimension of prepared laminate was: length 13·7 cm × width 2·3 cm × thickness 0·4 cm. These laminates were cut into specimen dimension according to ASTMD 2344. But, as the composite were prepared by hand lay technique and the specimens were cut by hacksaw, therefore the dimensions of the specimens were found with little differences. After getting the proper dimension, the fibre weight in the laminate were calculated as per the following equation (Thygesan 2006).

$$W_f = W_{f,start} \times \frac{l_c}{l_{f,start}}. \tag{14}$$

The matrix weight, W_m, was calculated based on W_c and W_f, where the subscript, m, denotes matrix.

$$W_m = W_c - W_f. \tag{15}$$

The volume fractions of the matrix, V_m and fibres, V_f were calculated based on the densities of the matrix, ρ_m and of the fibre, ρ_f. The values of ρ_m and ρ_f are 1·13 g/cc and 1·3 g/cc, respectively (Munikenche Gowda *et al* 1999; Mwaikambo 2002).

$$V_f = \frac{W_f}{\rho_f V_c}, \tag{16}$$

$$V_m = \frac{W_m}{\rho_m V_c}. \tag{17}$$

Assuming that on the macroscopic scale a composite material can be divided into two components, fibre and matrix, so the sum of the volume fraction for the two can be taken as 1. If the sum of the two exceeds 1 then the volume fraction of the porosity can be calculated as,

$$V_p = (V_f + V_m) - 1. \tag{18}$$

2.6c *Flexural 3-point bend test*: Composites test specimens were tested for their flexural strength under three-point bend tests in an Instron 1195 in accordance with ASTM standard D-790. A minimum of 10 composites samples for test were tested to account for statistical scatter and to arrive at the mean values. The entire test was carried out at room temperature.

For the test specimens with nominal dimensions of 130 × 25·4 × 4·8 mm, a span of 100 mm and a cross-head

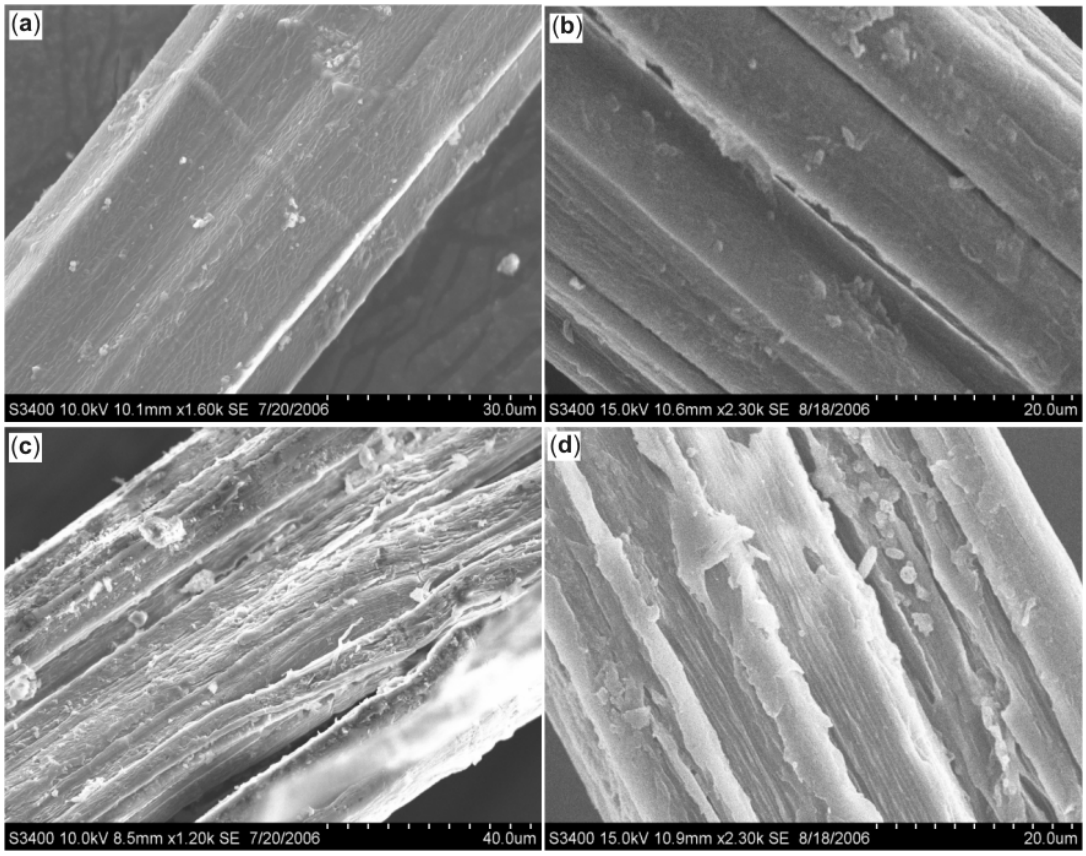

Figure 1. Surface morphology of different jute fibres: (**a**) raw jute, (**b**) M jute 2 h, (c) M jute 4 h and (**d**) M jute 8 h.

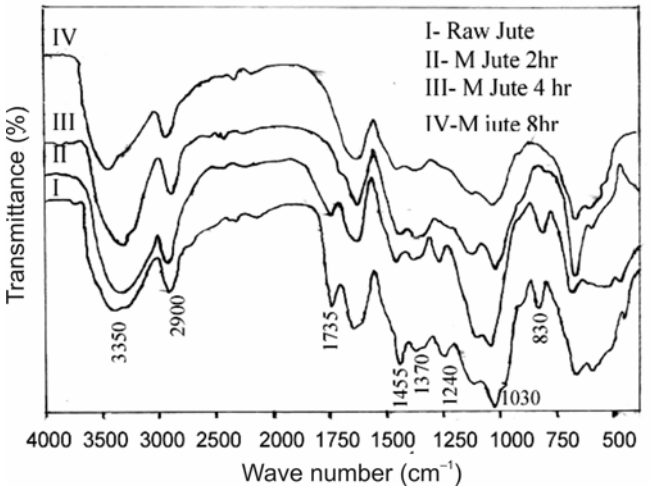

Figure 2. Infrared spectra of raw and alkali treated jute fibres.

speed of 2 mm/min were used. The applied load should be perpendicular to the fibre direction. Flexural strengths were determined by the formulae,

$$\sigma = \frac{1{\cdot}5 \times FL}{b \times d^2} \text{ MPa}, \tag{19}$$

where F is load, N, L the span length, mm, b the width of specimen, mm, d the thickness of specimen, mm, according to ASTM D790.

2.6d *Thermal analysis of composite*: DSC measurements of the composites were performed using a TA Instrument, USA, Model No. Q 10 thermal analyser. A heating rate of 10°C/min and a sample weight of 3–4 mg in an aluminum crucible with a pin hole were used in a nitrogen atmosphere (50 ml/min).

3. Results and discussion

3.1 *Surface topography studies of fibre by scanning electron microscope (SEM)*

The surface morphology of raw and mercerized jute fibres was analysed by scanning electron microscope (SEM).

Table 1. Absorbance intensity ratio of IR spectra of raw and alkali treated jute fibre.

Position of bands (cm^{-1})	Assignment	Raw jute (A_v/A_{2900})	M jute 2 h (A_v/A_{2900})	M jute 4 h (A_v/A_{2900})	M jute 8 h (A_v/A_{2900})
3350	H–O stretching (H bonded)	1·07	1·07	1·068	1·066
2900	C–H stretching in methyl and methylene	1·0 (0·11)	1·0 (0·158)	1·0 (0·073)	1·0 (0·114)
1735	C–O stretching in carbonyl and unconjugated β-ketone	1·023	0·548	nil	nil
1455	C–H deformation and CH_2 bending	1·09	0·92	0·75	shoulder
1370	C–H deforming (asymmetric)	1·093	0·987	nil	nil
1230–1240	C–O stretching in acetyl group	1·102	0·993	nil	nil
1030	Aromatic C–H in plane deformation	1·45	1·4	1·3	1·28
830	Aromatic C–H out-of-plane vibration	0·2	0·151	shoulder	shoulder

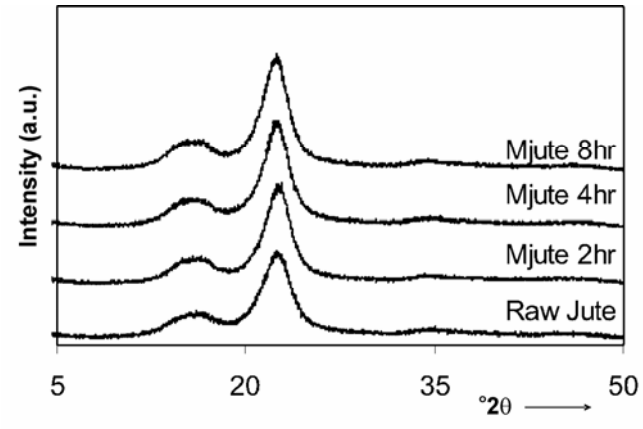

Figure 3. X-ray diffraction pattern of jute fibre samples before and after alkali treatment.

The SEM pictures of both raw and mercerized surfaces are shown in figure 1. The surfaces of raw jute were found to be smooth and showed their multicellular nature, whereas rough surface morphology and fragments on the surface of the mercerized jute fibre were observed (figure 1). It is also found that roughness increases as the treating time increases. The rough surface morphology was typical for the treated fibres, because of the removal of lignin and hemicelluloses and other structural effects (Gassan and Bledzki 1999). Thus, alkali treatment result in significant change of morphology of the fibre surface and is effective for available contact between fibre and polymatrix.

3.2 *FT–IR analysis of fibre*

IR spectra of the raw and alkali treated jute are shown in figure 2 from wave number 4000 to 450 cm^{-1}. The characteristic features of the spectrum of the jute are due to its constituents lignin, hemicelluloses and α-cellulose (Khan *et al* 2005). The 2900 cm^{-1} band has been chosen as an internal standard, as it is present as a prominent peak in the IR spectra of raw and alkali-treated jute fibres. This internal standard, though not fully established, has been adopted for making a comparative study of the spectra. The summary of the results, including the significance of the bands, the ratios of absorbance maxima of individual bands, and the 2900 cm^{-1} band (A_v/A_{2900}) are recorded in table 1. The 3350 cm^{-1} band, ascribed to H-bonded H–O stretching (Tshboi 1957), had almost the same absorbance intensity ratio for the alkali-treated jute samples and raw jute fibre. This finding is in concurrence with the almost constant α-cellulose contents even after mercerization of the jute fibres, as shown in table 1. The 2900 cm^{-1} is assigned to C–H stretching in methyl and methylene groups (Tshboi 1957). The band near 1735 cm^{-1} which is assigned to the C–O stretching of the carboxyl and acetyl groups in hemicelluloses of the jute fibre (Liang *et al* 1960), was prominent in raw jute fibre. This was found weak after 2 h and absent after 4 h alkali treatment, as shown in table 1. This can be explained on the basis of removal of hemicelluloses after alkali treatment, which is mainly due to the removal of acetyl group present in hemicelluloses after alkali treatment (Sarkar and Mazumdar 1955). The absorbance at 1455 cm^{-1} is attributed to CH_3 deformation (asymmetric) in lignin. The absorption intensity ratios were found to decrease after alkali treatment of jute fibre. This may be due to the loss of lignin after alkali treatment. The band at 1370 cm^{-1}, which is ascribed to the C–H deforming (symmetric), may be attributed to lignin, α-cellulose, or xylan, was found with higher absorption ratio for raw jute in comparison to the alkali-treated jute. The medium band at 1240 cm^{-1}, ascribed to C–O stretching in acetyl in xylan, was found prominent in raw jute, but decreases with alkali treatment due to the removal of acetyl group present in the hemicelluloses. The band at 1030 cm^{-1}, which is assigned to aromatic C–H– in plane deformation and C–O deformation for primary alcohol in lignin, was found with higher absorption intensity ratio in raw jute compared to alkali-treated fibre. This observation may be ascribed to the loss of lignin from the fibre after alkali treatment. The 830 cm^{-1} band which is assigned to the aromatic C–H out of phase vibration in lignin was found with higher absorbance intensity for raw jute fibre as compared to the alkali-treated jute.

Table 2. The observed and calculated parameters from the X-ray diffraction pattern.

Parameters	Raw jute	M jute 2h	M jute 4 h	M jute 8 h
Peak position (2θ)	22·5	22·48	22·46	22·44
FWHM (2θ)	2·772	2·437	2·424	2·402
d (Å)	3·942	3·950	3·954	3·957
Crystallite size (Å)	29·25	33·26	33·32	33·63
ε	0	0·002	0·003	0·004
I_{002} (counts/s)	1664	1836	1974	2102
I_{am} (counts/s)	569	554	585	615
CrI (%)	65·80	68·81	70·36	70·74
σ_{stress} (10^{-4}) (N/tex)	0	1·12	1·68	2·24

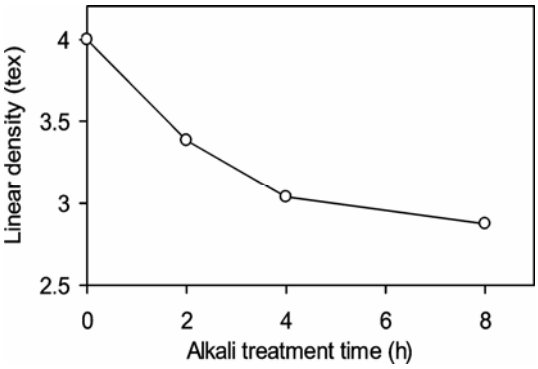

Figure 4. The variation of linear density with alkali treatment time.

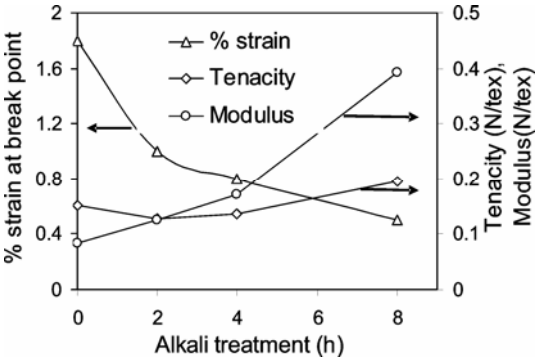

Figure 5. The variation of strain at break point, tenacity and modulus of the fibre with alkali treatment period.

3.3 *XRD studies on fibres*

Figure 3 shows the room temperature X-ray diffraction pattern of raw jute fibre samples before and after alkali treatment for 2 h, 4 h and 8 h. The pattern shows the 002 peak slightly shifting towards lower angle indicating the increase in d spacing. The microstress and percentage crystallinity are also calculated from the diffractogram and presented in table 2.

From the table it is clear that the FWHM of diffraction peak decreases after alkali treatment. The degree of crystallinity (CrI%), using the Segal empirical method was found to increase after alkali treatment. Ray and co-workers (2001) also reported similar observation. The extent of crystallinity formation by NaOH treatment was also determined from the improvement in the intensity of the peaks (Ray *et al* 2001). Table 2 shows that degree of crystallinity increases after alkali treatment. This may be due to the formation of new hydrogen bonds between certain of the cellulose chains as a result of the removal of hemicelluloses, which normally separates the cellulose chains (Ray *et al* 2001).

3.4 *Mechanical properties analysis of the fibre*

Figure 4 shows the variation of linear density (tex) of the fibre with alkali treatment time. The figure shows a decreasing trend of the tex with treatment time. In the present case, linear densities of the fibres decrease from 4 to 2·8, from raw jute to 8 h alkali treated jute, respectively. Figure 5 shows the variation of strain at break point, tenacity and modulus of the fibre with alkali treatment period. The figure shows that the modulus increased by 33% at 2 h of treatment, after which the increase was by 50% and 78% for 4 h and 8 h treatments, respectively. Tenacity at break decreased after 2 h treatment, but was found to increase by nearly 22·5% after 8 h treatment. Percent (%) breaking strain was reduced by 44% after 2 h treatment, whereas the reduction was 55·5% and 72·2% after 4 h and 8 h treatments, respectively. Thus, the results show that alkali-treated fibres were stiffer and brittle in comparison to raw fibres, as reported for *Corchorus capsularies* (Ray *et al* 2001). In untreated jute fibres, hemicelluloses and lignin remain dispersed in the interfibrillar region separating the cellulose chain from one another. The cellulose chains are, therefore, always in a state of constraint. Removal of hemicelluloses and lignin after alkali treatment, removed internal constraint and the fibrils became more capable of rearranging themselves in a compact manner, leading to a closer packing of the cellulose chain, which causes improvement in fibre strength and its mechanical properties. This is also responsible for the increase in the crystallinity of the fibre after alkali treatment as supported by our XRD analysis.

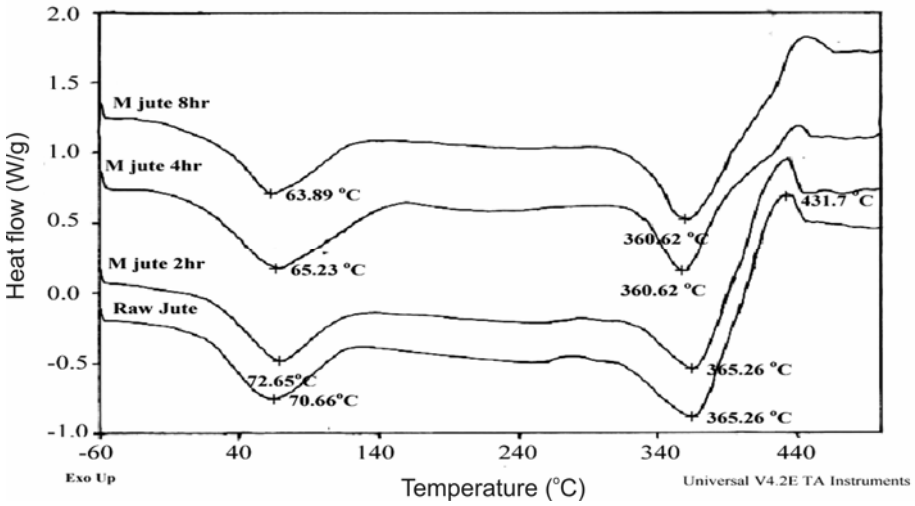

Figure 6. DSC thermogram of raw and alkali treated jute fibre.

Table 3. Water uptake capacity of the jute fibre/UPE composite.

Sample details	Dry weight (W_1) (g)	Immersed weight (W_2) (g)	Water uptake (%)
Raw jute/UPE composite	4·04	4·20	3·9
M jute 2 h/UPE composite	4·02	4·10	1·9
M jute 4 h/UPE composite	3·91	3·95	1·2
M jute 8 h/UPE composite	4·00	4·02	0·5

3.5 *Thermal properties analysis of fibre*

Differential scanning calorimetric (DSC) analysis was carried out on the raw and alkali treated jute fibres to determine the thermal behaviour of fibre. DSC analysis also enables the identification to be made of chemical activity occurring in the fibres as the temperature is increased.

DSC analysis curve of raw and alkali treated jute fibres are shown in figure 6. A broad endothermic peak observed in the temperature range of 60–140°C in both alkali treated and raw jute corresponds to the heat of vapourization of water absorbed in the fibres. It is reported (Aziz and Ansell 2004) that in cellulose fibres, lignin degrades at a temperature around 200°C while the other polysaccharides such as cellulose degrades at higher temperature. Therefore, the peaks which are at higher temperature than 200°C indicates the decomposition of cellulose in the fibres. The region between 150 and 240°C shows no exothermic or endothermic reactions, which suggest that the fibres are stable between these temperatures. The first exothermic hump in the DSC curve for raw jute fibre is about 290·2°C which is due to the thermal degradation of hemicellulose and the glycosidic linkages of cellulose. The very strong second endothermic peak at about 365·26°C indicates the degradation of cellulose, leading to the formation of char. In addition, there is one more step with a peak at 431·7°C. In this step, the rest of the char is oxidized and the rest of the mass consumed (Paunikallio *et al* 2001). In the DSC curve for different alkali treated jute fibres, it is found that the exothermic hump for decomposition of hemicellulose are very weak after 2 h alkali treatment and almost missing after 4 h and 8 h alkali treatments. This may be due to the removal of hemicellulose from the fibre after alkali treatment. According to the second endothermic peak, it can be deduced that the degradation peak of the cellulose shifted to lower temperature, 360·62°C from 365·26°C after 4 h and 8 h alkali treatments. This lowering of the decomposition temperature leads to the reduction in the thermal stability of alkali-treated fibres. Dipa Ray and coworkers (2002) also reported the same.

3.6 *Water absorption analysis of composites*

Water absorption capacities of the raw and alkali treated jute fibre composites were calculated using (12). Table 3 shows the dry weight, immersed weight and water uptake percentage of the composites. It shows a decrease in water uptake capability of the alkali treated jute fibre reinforced composite. This may be due to the effect of alkaline solubilization of hemicelluloses which are usually ascribed to the destruction and breaking of hydrogen bonds. In particular, all the ester-linked substances of the hemicelluloses can be cleaved by alkali except for the cleavage of

Table 4. Physical dimension of the test specimen along with the volume fraction of porosity.

Sample details	l_c (cm)	t_c (cm)	b_c (cm)	W_c (g)	$W_{f,start}$ (g)	W_f (g)	W_m (g)	V_f (cm^3)	V_m (cm^3)	V_p (cm^3)
Raw jute/UPE composite	4·2	0·48	0·65	2·088	2·3	0·705	1·3839	0·417	0·935	0·352
M jute 2 h/UPE composite	4·2	0·47	0·60	1·852	2·3	0·705	1·1470	0·400	0·775	0·175
M jute 4 h/UPE composite	4·2	0·47	0·60	1·652	2·3	0·705	0·9470	0·400	0·630	0·030
M jute 8 h/UPE composite	4·2	0·47	0·60	1·526	2·3	0·705	0·9320	0·400	0·620	0·020

Table 5. Flexural properties of composites reinforced with untreated and alkali-treated jute fibres (SD = Standard deviation).

	Flexural strength (MPa)	
Sample ID	Mean value	S.D.
Raw jute composite	158·65	4·2
M jute 2 h composite	163·66	2·5
M jute 4 h composite	173·68	5·8
M jute 8 h composite	132·93	3·6

α-ether bonds between lignin and hemicelluloses. This tends to increase hydrophobicity and hence solubility of the polymer (Uraki *et al* 1997).

3.7 *Determination of volume fraction of porosity V_p in the composites*

The volume fraction of porosity of the raw and alkali treated jute fibre composites, which was prepared according to ASTMD 2344 were calculated using (13)–(18). Physical dimension, fibre weight in the laminate, the matrix weight, volume fraction of fibre and matrix and volume fraction of porosity of the raw and alkali treated jute fibre composite are shown in table 4. In natural fibre-reinforced polymer composites due to the divergent behaviour in polarity, i.e. natural fibres are hydrophilic, whereas most of the polymers are hydrophobic, fibre to matrix adhesion is poor. Incomplete wetting or impregnation often results in the formation of voids or air entrapments. Although the occurrence of voids has been frequently reported and is recognized as a major problem in composite, the exact mechanism of void formation is not clear due to its complexity (Bascom *et al* 1968).

Incomplete wetting will produce interfacial defects and thereby lower the adhesive bond strength, whereas good wetting enhances the adhesive bond strength.

Fibre surface treatment by alkali leads to the fibre fibrillation, i.e. breaking down of composite fibre bundles into smaller fibres. In addition to this alkali treatment improves the fibre surface adhesive characteristic by removing natural and artificial impurities, thereby producing a rough surface topography. This is observed in our SEM images for alkali treated fibres (figure 1). This roughness offers better fibres matrix interface adhesion (Ray *et al* 2002) and reduction in the volume fraction of porosity as compared to raw fibre composite.

3.8 *Mechanical property of fibre reinforced polymer composites*

The mechanical properties of composite prepared with raw and treated fibre with alkali (5% NaOH solution) are included in table 5. For each type of composite the value of the mechanical characteristic were the arithmetic means of atleast four different specimens. Breaking energy of the samples were calculated from the area under the curve load/displacement to the break point and the toughness was obtained by dividing the energy to break by the area to the test specimens.

The load displacement curves of the four varieties of the composites reinforced with 15 weight% of untreated, 2 h, 4 h and 8 h alkali-treated fibres are shown in figure 7. Heavy fibre pull-out and breakage was observed in raw fibre composite. These were found to decrease for alkali treated fibre composites, imperative of a better bonding at the interface between the fibre and the matrix. The mechanical properties of composite reinforced with 2h and 4h alkali-treated fibre were found to be superior in comparison to the untreated and 8h treated fibre reinforced (as shown in table 5) having increase in the flexural strength of 3·16% (shown in figure 7) after 2 h alkali-treated fibre composite compared to the untreated one, and the increase of 9·5% in flexural strength for 4 h alkali-treated fibre composite. The maximum improvement in strength was observed for composite prepared with 4 h-alkali treated fibre although 8 h treated fibres had superior fibre characteristics. Alkali treatment makes the fibre rigid and somewhat brittle afterwards owing to the development of crystallinity causing high strength and low extensibility. On the application of stress, these fibres suffered breakage due to increased brittleness and could not take part in effective stress transfer at the interface, thus lowering the strength of the composite (Ray *et al* 2001).

3.9 *Thermal analysis of raw and alkali-treated-jute fibre reinforced composites*

Figure 8 shows the thermal behaviour of the raw and treated jute fibre reinforced polymer composite. The detailed thermal responses of the composites were summarized in table 6. The inserted figure represents the DSC curve of the neat unsaturated polyester (UPE) which showed an exothermic peak at 398·20°C. The moisture desorption peak below 100°C was small and therefore, was neglected. The overall thermal degradation pattern of the UPE resin matrix composites reinforced with untreated and alkali-treated jute fibres was an additive contribution by the individual thermal degradation features of the two components: the matrix and the fibres. A slight endothermic moisture desorption peak at 71·3°C was observed below 100°C in the DSC curve of the composite reinforced with raw jute fibres. Water present in the composite originates largely from the fibre implying composites were not effectively pre-conditioned prior to the preparation of composite. But due to the pretreatment of the fibres by oven heating at 50°C for 8 h before the preparation of the composites has led to the reduction of moisture content of the fibre in our case. The small, broad exothermic hump observed at 290·2°C and sharp endothermic peak at 365·26°C were due to the degradation of the hemicelluloses and cellulose, respectively (Paunikallio *et al* 2004) in the fibre part of the composite. The strong, sharp exothermic peak at 398·3°C was due to the degradation of the resin part of the composites.

In the composite reinforced with alkali-treated jute fibre, the moisture loss peak shifted to higher temperature, from 71·3°C for the untreated-fibre-reinforced composite to 78·4°C after the 8 h-alkali-treated-fibre reinforced composites. This tendency of releasing moisture at a higher temperature in the treated composite could be due to the improved wetting of the finely separated fibres by the resins, resulting in the reduction of the available surface area required for the moisture desorption through a decay in the moisture evaporation (Ray *et al* 2004). The hemicellulose degradation temperature was found almost the same for all composites. The cellulose degradation temperature in the fibre part of the composites increased from 365·26°C for raw fibre reinforced composite to 367·92°C for 4 h-alkali-treated fibre composite and to 368·4°C for 8 h-alkali-treated fibre composite. The main degradation temperatures of the resin part in the composite remain almost constant. The increased degradation temperature of the cellulose of the alkali-treated-fibre composite as compared to the untreated-jute-composites indicated that the closely packed cellulose chain resists the thermal degradation in combination with the resin. This was indicative of the increased thermal stability of the treated composites.

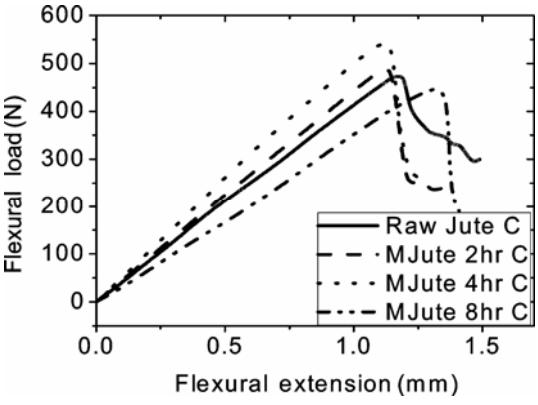

Figure 7. Load displacement curves for the untreated and treated fibre reinforced polymer composite.

4. Conclusions

Jute fibres (*Corchorus olitorius*) were treated with 5% NaOH for 2 h, 4 h and 8 h. From FT–IR spectra, it is revealed that the bands 1735, 1370, 1230–1240, 1030 cm^{-1} and the band at 1455 and 830 cm^{-1} ascribed mainly to hemicelluloses and to the lignin, show higher absorbance intensity ratio for the raw jute in comparison to the alkali-treated jute. This finding can be attributed to the loss of the hemicelluloses and lignin after alkali treatment. SEM study shows that the surface morphology of the fibre becomes rough after alkali treatment and roughness increases with increase in the treatment period due to the removal of hemicelluloses and lignin. The removal of hemicelluloses and lignin from the cell of the fibre releases the internal constraint and the fibrils become more capable of rearranging themselves in a compact manner, leading to the closer packing of the cellulose.

Table 6. DSC analysis of raw and alkali treated fibre reinforced composites.

Sample details	Peak temperature (°C)	Nature of peak
Raw jute/UPE composite	71·3	endo
	290·2	exo
	365·26	endo
	398·3	exo
M jute 2 h/UPE composite	72·6	endo
	290·2	exo
	365·26	endo
	398·3	exo
M jute 4 h/UPE composite	75·3	endo
	290·2	exo
	367·92	endo
	398·25	exo
M jute 8 h/UPE composite	75·3	endo
	290·2	exo
	367·92	endo
	398·2	exo

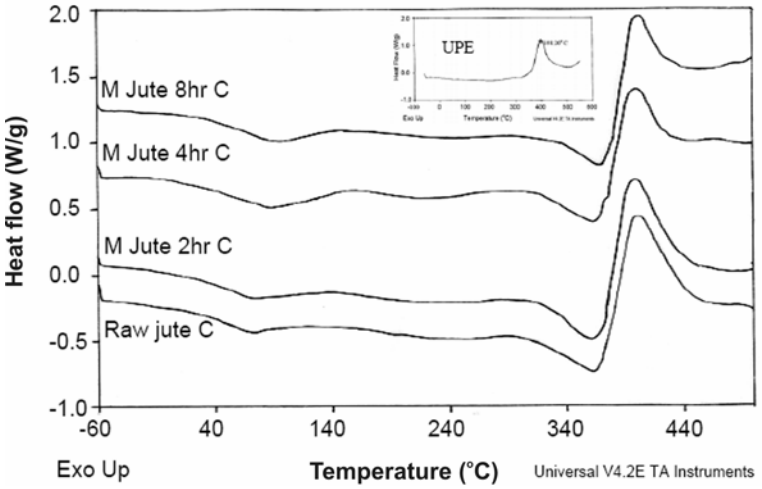

Figure 8. DSC curves of composite reinforced with raw and alkali treated jute fibre.

This closer packing of the cellulose also improves the crystallinity of the fibre after alkali treatment as evidenced by our XRD analysis. The average value of the tenacity of the fibres is found to increase after alkali treatment due to the improvement in the crystallinity of the fibre with a drop at 2 h alkali treatment. This drop may be due to the heavy dissolution of the hemicelluloses and little that of lignin, primarily within 2 h of the treatment. The DSC analysis showed that the thermal stability of the jute fibre reduces after alkali treatment.

Mercerization helps in the development of hydrophobicity on to the fibre and thus reduces the water uptake capacity of the alkali treated fibre composite. This may be due to the effect of alkaline solubilization of hemicelluloses which are usually ascribed to the destruction and breaking of hydrogen bonds. In particular, all the ester-linked substances of the hemicelluloses can be cleaved by alkali except for the cleavage of α-ether bonds between lignin and hemicelluloses. This tends to increase hydrophobicity. Volume fraction of the porosity is also found to reduce for alkali treated jute fibre composite as compared to the raw fibre composite. This may be due to fibre fibrillation, i.e. breaking down of composite fibre bundles into smaller fibres caused by alkali treatment. In addition to this alkali treatment improves the fibre surface adhesive characteristic by removing natural and artificial impurities, thereby producing a rough surface topography. This is also observed in our SEM study of alkali treated fibres. This roughness offers better fibres matrix interface adhesion and reduction in the volume fraction of porosity as compared to raw fibre composite. The composite prepared with jute fibre treated for 2 h and 4 h with 5% NaOH solution shows improvement in the flexural mechanical properties due to the better bonding at the interface between fibre and matrix. Flexural strength of the composite prepared with 2 h and 4 h alkali treated fibre are found to increase by 3·6% and 14·8%, respectively. Although 8 h treated fibre exhibited maximum strength properties, but the composite prepared with them showed lower strength value. This is due to the fibre surface treatment by alkali which makes the fibre stiff due to the development of crystallinity in fibre and brittle which accounts for its high strength and low extensibility. On the application of stress, these fibres suffered breakage due to increased brittleness and could not take part in effective stress transfer at the interface, thus lowering the strength of the composite. DSC analysis of the composite showed that the cellulose degradation temperature in the fibre part of the composites increased from 365·26°C for raw fibre reinforced composite to 367·92°C for 4 h-alkali-treated fibre composite and to 368·4°C for 8 h-alkali-treated fibre composite. The main degradation temperature of the resin part in the composite was almost found the same. The increased degradation temperature of the cellulose of the alkali-treated-fibre composite as compared to the untreated-jute-composites indicated that the closely packed cellulose chain resists the thermal degradation in combination with the resin. This was indicative of the increased thermal stability of the treated composites.

References

Aziz S H and Ansell M P 2004 *Compos. Sci. Technol.* **64** 1219

Bascom W D and Romans J B 1968 *Ind. Eng. Chem. Prod. Res. Dev.* **7** 172

Bledzki A K, Reihmane S and Gassan J 1996 *J. Appl. Polym. Sci.* **59** 1329

Cullity B D 1978 *Elements of X-ray diffraction* (London: Addison Wesley Publishing Company Inc) p. 286

Gassan J and Bledzki A K 1999 *Compos. Sci. & Technol.* **59** 1303

Khan F and Ahmed S R 1996 *Polym. Degrad. & Stab.* **52** 335
Khan M A, Hassan M M and Drza L T 2005 *Composites: Part A* **36** 71
Liang C Y, Bassett K H, McGinnes E A and Marchessault R H 1960 *Tappi* **43** 1917
McMillan W G, Sen Gupta A B and Majumdar S K 1954 *J. Textile Inst.* **45** T703
Mohanty S, Nayak S K, Verma S K and Tripathy S S 2004 *J. Reinf. Plast. & Compos.* **23** 2047
Munikenche Gowda T, Naidu A C B and Chhaya Rajput 1999 *Composite: Part A* **30** 277
Mwaikambo L 2002 *Plant based resources for sustainable composites*, Ph.D thesis, Department of Engineering and Applied Science, University of Bath
Paunikallio T, Suvanto M and Pakkanen T T 2004 *J. Appl. Polym. Sci.* **91** 2676
Porod G 1953 *Kolloid Z. Z. Polym.* **133** 16
Prasad S V, Pavithran C and Rohatgi P K 1983 *J. Mater. Sci.* **18** 1443
Ratho T and Sahu N C 1970 *Kolloid Z.Z. Polym.* **236** 43
Ray D, Sarkar B K, Rana A K and Bose N R 2001 *Composites: Part A* **32** 119
Ray Dipa, Sarkar B K, Basak R K and Rana A K 2002 *J. Appl. Polym. Sci.* **85** 2594
Ray Dipa, Sarkar B, Basak R K and Rana A K 2004 *J. Appl. Polym. Sci.* **94** 123
Rout J, Mishra M, Nayak S K, Tripathy S S and Mohanty A K 1999 *Poly. Beyond AD 2000* 489
Roy S C 1960 *Text. Res. J.* **30** 451
Samal R K, Mohanty M and Panda B B 1995 *J. Polym. Mater.* **12** 235
Sarkar P B 1935 *Indian J. Chem. Soc.* **12** 23
Sarkar P B and Mazumdar A K 1955 *Text. Res. J.* **12** 1016
Segal L, Creely J and Martin Conrad C M 1959 *Text. Res. J.* **29** 786
Thygesen Anders 2006 *Properties of hemp fibre polymer composites*, Ph.D thesis, Rise National Laboratory, Denmark
Tshboi M 1957 *J. Polym. Sci.* **25** 159
Uraki Y, Hashida K and Sano Y 1997 *Holzforschung* **51** 91